ФИЗИКА

УДК 535.016

РЕЗОНАНСНОЕ ПЬЕЗОФОТОАКУСТИЧЕСКОЕ ПРЕОБРАЗОВАНИЕ БЕССЕЛЕВЫХ СВЕТОВЫХ ПУЧКОВ В ПЛОТНОМ СЛОЕ УГЛЕРОДНЫХ НАНОТРУБОК

Г.С. Митюрич[1], **Е.В. Лебедева**[2], **А.Н. Сердюков**[1]

[1]*Гомельский государственный университет им. Ф. Скорины*
[2]*Белорусский торгово-экономический университет потребительской кооперации, Гомель*

RESONANCE PIEZOPHOTOACOUSTIC TRANSFORMATION OF BESSEL LIGHT BEAMS IN DENSE LAYER OF CARBON NANOTUBES

G.S. Mityurich[1], **E.V. Lebedeva**[2], **A.N. Serdyukov**[1]

[1]*F. Scorina Gomel State University*
[2]*Belarusian Trade and Economics University of Consumer Cooperatives, Gomel*

Исследовано явление возникновения фотоакустического сигнала в слое углеродных нанотрубок под действием облучения бесселевыми световыми пучками (БСП) для случая пьезоэлектрической регистрации. Установлено, что увеличение угла конусности БСП влияет на частоту появления резонансных пиков в зависимости от радиальной координаты ρ.

***Ключевые слова**: фотоакустическое преобразование, пьезоэлектрическая детекция, плотный слой углеродных нанотрубок, бесселевы световые пучки, скорость диссипации энергии, амплитуда фотоакустического сигнала, функция Бесселя, уравнение теплопроводности.*

The phenomenon of the appearance of a photoacoustic signal in a layer of carbon nanotubes under the action of irradiation with Bessel light beams (BLB) is studied for the case of piezoelectric recording. It was found that an increase in the taper angle of BLB affects the frequency of occurrence of resonance peaks depending on the radial coordinate ρ.

***Keywords**: photoacoustic transformation, piezoelectric detection, dense layer of carbon nanotubes, Bessel light beams, energy dissipation rate, amplitude of photoacoustic signal, Bessel function, heat equation.*

Introduction

Bessel light beams (BLB) are used and widely used in laser photoacoustic methods to diagnose the structure of various samples as a source of sound excitation [1]–[4]. In particular, the use of Bessel light beams in optical-acoustic microscopy makes it possible to effectively increase the focal depth of the resulting photoacoustic image in comparison with a conventional Gaussian light beam. The use of different types of BLB polarization modes is explained by the fact that BLBs have a number of unique properties, for example, non-diffraction of propagation in space.

Promising material in various fields of science and technology are carbon nanotubes (CNTs). One of the main advantages of these structures is the ability to control the properties of the created CNT layers [5] by changing the geometric dimensions and configuration of nanoobjects.

The classical theory of electrodynamics can not always be applied to the description of nanotubes. Consequently, it is required to search for new quasi-classical theoretical approaches and studies that would enable us to solve the problems of micro- and macroscopic electrodynamics [6], which underlie the theoretical basis of modern photoacoustic spectroscopy.

This paper is devoted to the construction of a model of photoacoustic conversion of BLB modes in a layer of chiral and achiral carbon nanotubes for the case of piezoelectric recording of the resultant signal.

1 Conductivity of chiral and achiral carbon nanotubes

The electronic structure of carbon nanotubes is described in the π-electron Hückel approximation [7] and in the general case within the framework of the tight-binding method using the nearest-neighbor approximation, is expressed by the well-known relation [8]:

$$\varepsilon(\vec{p}) = \pm\gamma_0\left(1+4\cos\left(\vec{p}\frac{\vec{a}_1+\vec{a}_2}{2\hbar}\right)\cos\left(\vec{p}\frac{\vec{a}_1-\vec{a}_2}{2\hbar}\right)+4\cos^2\left(\vec{p}\frac{\vec{a}_1-\vec{a}_2}{2\hbar}\right)\right)^{\frac{1}{2}}. \quad (1.1)$$

The modulus of the chirality vector of carbon nanotubes is determined by the ratio

$$\left|\vec{C}_h\right| = a\sqrt{n^2+nm+m^2}. \quad (1.2)$$

The projections of the momentum vector on the *Ox* and *Oy* axes of the Cartesian coordinate system for chiral carbon nanotubes are determined in accordance with the following equalities

$$\vec{p}\frac{\vec{a}_1+\vec{a}_2}{2\hbar} = \frac{1}{l}\left(\frac{3\pi q_1(n+m)}{2l}+\frac{\sqrt{3}a(n-m)}{4\hbar}p_y\right), \quad (1.3)$$

$$\vec{p}\,\frac{\vec{a}_1-\vec{a}_2}{2\hbar}=\frac{1}{l}\left(\frac{\pi q_1(n-m)}{2l}+\frac{\sqrt{3}\,a(n+m)}{4\hbar}p_y\right), \quad (1.4)$$

where $l=\sqrt{n^2+nm+m^2}$, $q_1=1,2,\ldots,l$.

Taking into account (1.3) and (1.4) in expression (1.1), we carry out the transition to cylindrical coordinates ($p_x \to p_\varphi, p_y \to p_z$). After transformations, we obtain the following expression for describing the electronic structure of carbon nanotubes:

$$\varepsilon(\vec{p})=\pm\gamma_0\times$$
$$\times\left[1+4\cos\left(\frac{1}{l}\left(\frac{3\pi q(n+m)}{2l}+\frac{\sqrt{3}a(n-m)}{4\hbar}p_z\right)\right)\times\right.$$
$$\times\cos\left(\frac{1}{l}\left(\frac{\pi q(n-m)}{2l}+\frac{\sqrt{3}a(n+m)}{4\hbar}p_z\right)\right)+ \quad (1.5)$$
$$\left.+4\cos^2\frac{1}{l}\left(\frac{\pi q(n-m)}{2l}+\frac{\sqrt{3}a(n+m)}{4\hbar}p_z\right)\right]^{1/2}.$$

We find the projection of the electron velocity vector onto the z axis as a partial derivative of function (5) with respect to the variable p_z

$$\upsilon(p_z)=\frac{\partial\varepsilon(\vec{p})}{\partial p_z}. \quad (1.6)$$

Taking into account relations (1.5) and (1.6), we obtain an expression for the projection of the velocity

$$\upsilon(p_z)=\frac{\pm\sqrt{3}\gamma_0 a\left[m\sin(\psi_1-\psi_2)-\right.}{\left.-n\sin(\psi_1+\psi_2)-(n+m)\sin 2\psi_2\right]}{\hbar l\left(1+4\cos\psi_1\cos\psi_2+4\cos^2\psi_2\right)}, \quad (1.7)$$

where

$$\psi_1(p_z)=\frac{1}{l}\left(\frac{3\pi q(n+m)}{2l}+\frac{\sqrt{3}\,a(n-m)}{4\hbar}p_z\right); \quad (1.8)$$

$$\psi_1(p_z)=\frac{1}{l}\left(\frac{\pi q(n-m)}{2l}+\frac{\sqrt{3}a(n+m)}{4\hbar}p_z\right). \quad (1.9)$$

Next, we consider the Boltzmann equation describing the motion of π-electrons over the cylindrical surface of a single-walled nanotube in the semiclassical approximation [9]:

$$\frac{\partial f}{\partial t}+eE_z\frac{\partial f}{\partial p_z}+\nu_z\frac{\partial f}{\partial z}=J\left(F(\vec{p});f(\vec{p},z,t)\right), \quad (1.10)$$

where e is charge of electron; $\nu_z=\partial\varepsilon(\vec{p})/\partial p_z$ – speed of electron; $J(F,f)$ – integral of clash; $F(\vec{p})=1/\left[1+\exp\left(\varepsilon(\vec{p})/k_BT\right)\right]$ is the equilibrium Fermi distribution function; T – temperature; k_B – Boltzmann constant.

To calculate the integral of clash, we use the relaxation time approximation, according to which

$$J\left(F(\vec{p});f(\vec{p},z,t)\right)\cong\nu\left[F(\vec{p})-f(\vec{p},z,t)\right],$$

where $\nu=1/\tau$ is the frequency of relaxation; τ – mean free path of an electron.

The limitation imposed on the semiclassical model for describing the motion of an electron along the surface of a CNT from the side of high frequencies can be written as follows:

$$\omega<\omega_l, \quad (1.11)$$

where $\omega_l=2\nu_F/R_n$ corresponds to metal nanotubes, $\omega_l=2\nu_F/3R_{cn}$ – to semiconductor nanotubes; $v_F=a\gamma_0$ is the speed of π-electrons at the Fermi level; R_{cn} – radius of nanotube.

Further, the semiclassical model is used to calculate the axial current in a straight infinitely long nanotube, which arises under the action of the electric field of a traveling wave

$$E_z=\mathrm{Re}\left[E_z^0\exp\left(i\left(hz-\omega t\right)\right)\right],$$

where h is a constant of spread.

Let's find a small pertubation δf from equation (10) by an approximation linear in the field, taking into account that $E_z=F+\mathrm{Re}\left[\delta f\exp\left(i\left(hz-\omega t\right)\right)\right]$:

$$\delta f=-i\frac{\partial F}{\partial p_z}\frac{eE_z^0}{\omega-h\nu_z+i\nu}.$$

Then the surface axial current

$$j_z=\mathrm{Re}\left[j_z^0\exp\left(i\left(hz-\omega t\right)\right)\right]$$

density can be determined by integrating the following equality

$$j_z=\frac{2e}{(2\pi\hbar)^2}\iint\nu_z f d^2\vec{p}. \quad (1.12)$$

Expression (1.12) can be represented in a more compact form $j_z^0=\sigma_{zz}(h,\omega)E_z^0$, where σ_{zz} is a axial conductivity of a nanotube, which can be defined as follows:

$$\sigma_{zz}(h,\omega)=\frac{2e}{(2\pi\hbar)^2}\iint\frac{\partial F}{\partial p_z}\frac{\nu_z d^2\vec{p}}{\omega-h\nu_z+i\nu}. \quad (1.13)$$

Taking into account expressions (1.13) and (1.7), we calculate the axial electrical conductivity of chiral nanotubes:

$$\sigma_{zz}(\omega)=-\frac{ie^2}{\pi\hbar l}\frac{1}{(\omega+i\nu)}\sum_{s=1}^{m}\int_{-P_0}^{P_0}\upsilon_z^2(p_z,s)\frac{\partial F}{\partial\varepsilon}dp_z, \quad (1.14)$$

where $P_0=\dfrac{2\pi\hbar}{\sqrt{3}bl}$,

$$\frac{\partial F}{\partial\varepsilon}=\frac{\exp(\varepsilon/k_BT)}{k_BT\left[1+\exp(\varepsilon/k_BT)\right]^2}.$$

By analogy with [6], the conductivity of chiral CNTs in cylindrical coordinates is determined by the relation, (electron velocity $v_e \ll c$, c – speed of light)

$$\sigma_{zz}(\omega)=-\frac{2P_0ie^2}{\pi\hbar l}\frac{1}{(\omega+i\nu)}\sum_{s=1}^{m}\upsilon_z^2(p_z,s)\frac{\partial F}{\partial\varepsilon}, \quad (1.15)$$

For CNTs of the zigzag type, the expressions for the axial conductivity are expressed by the formula

$$\left|\sigma_{zz}(\omega)\right| = \frac{2w_{cn}e^2P_0}{\sqrt{3}\pi^2R_{cn}\sqrt{\left(\omega^2+\nu^2\right)}k_BT}\sum_{S=1}^{m}\frac{\exp\left(\varepsilon_0/k_BT\right)}{\left[1+\exp\left(\varepsilon_0/k_BT\right)\right]^2},$$

$$\varepsilon_0 = \varepsilon\left(P_0\right) = \gamma\sqrt{1+4\cos\left(aP_0\right)\cos\left(\frac{\pi S}{m}\right)+4\cos^2\left(\frac{\pi S}{m}\right)}.$$

Also obtained expression describing the axial conductivity in carbon nanotubes armchair type

$$\left|\sigma_{zz}(\omega)\right| = \frac{2w_{cn}e^2P_0}{\pi^2R_{cn}\sqrt{\left(\omega^2+\nu^2\right)}k_BT}\sum_{S=1}^{m}\frac{\exp\left(\varepsilon_0/k_BT\right)}{\left[1+\exp\left(\varepsilon_0/k_BT\right)\right]^2},$$

$$\varepsilon_0 = \varepsilon\left(P_0\right) = \gamma\sqrt{1+4\cos\left(\frac{a\hbar S}{R_0}\right)\cos\left(\frac{aP_0}{\sqrt{3}}\right)+4\cos^2\left(\frac{aP_0}{\sqrt{3}}\right)}.$$

The expression for the projection of the electron velocity vector on the z axis is obtained with allowance for the formula $\upsilon(p_z) = \partial\varepsilon(\mathrm{p})/\partial p_z$ [10] and the relationship for the energy distribution within the tight-binding approximation, which takes into account the interaction of only the nearest neighboring atoms in the hexagonal structure [11], [12].

2 Dissipation of energy of Bessel light beams in chiral and achiral carbon nanotubes

The effect of a Bessel light beam on the absorbing layer of chiral nanotubes leads to a periodic change in the temperature field, which can be described by the equation of thermal conductivity

$$\nabla^2T - \frac{1}{\beta_S}\frac{\partial T}{\partial t} = -\frac{1}{2k_S}Q\left(1+e^{i\Omega t}\right), \qquad (2.1)$$

where $\beta_s = k_S/\rho_0\cdot C$ is effective coefficient of thermal diffusivity, k_S is coefficient of thermal conductivity, ρ_0 is density of a layer of carbon nanotubes, C is specific heat of a layer of CNTs, Ω is modulation frequency.

In equation (2.1) Q is volume density of thermal sources, which is determined by the expression

$$Q = \sigma_{cn}\left|E\right|^2, \qquad (2.2)$$

where $|\sigma_{cn}| = 2\pi\cdot|\sigma_{zz}|/\lambda$ is conductivity of the CNT layer. Substituting into (2.2) the relation describing the intensity of the wave, it is easy to obtain the energy dissipation rate

$$Q = 2\alpha_0I_0e^{-2\alpha_{eff}z} = 2\sigma_{cn}/(c\sqrt{\varepsilon'}\varepsilon_0)I_0e^{-2\alpha_{eff}z}. \qquad (2.3)$$

In the formula (2.3) I_0 is Proceeding from the geometry of chiral and achiral carbon nanotubes, it is expedient to write equation (2.1) in a cylindrical coordinate system. The absorption coefficient in (2.2) is defined as follows

$$\alpha_0 = (\omega/c)\cdot\left(\varepsilon''/\sqrt{\varepsilon'}\right) = (\omega/c)\cdot(\varepsilon''/n).$$

Conductivity is related to the imaginary part of the dielectric constant by the formula $\varepsilon = \varepsilon' + i\varepsilon''$, $\varepsilon'' = \sigma/\omega\varepsilon_0$ ($\varepsilon_0 = 8{,}85\cdot10^{-12}\,f/m$).

Thus, in cylindrical coordinates, the energy dissipation rate of Bessel light beams (BLB) in the layer of absorbing carbon chiral nanotubes can be represented as follows

$$Q^{TE} = \frac{2\left|\sigma_{cn}\right|I_0}{c\sqrt{\varepsilon'}\varepsilon_0}\frac{c}{4\pi}k_0\varepsilon_\alpha\left(n_1^2+n_2^2\right)\times \left[\frac{m^2}{(q\rho)^2}J_m^2(qr)+J_m'^2(qr)\right]\exp(-\alpha_{eff}z), \qquad (2.4)$$

where $\alpha = 2k_{zz}$.

3 Calculation of the resulting photoacoustic signal

Let us determine the amplitude of the photoacoustic signal arising in the layer of chiral CNTs upon irradiation by the TE mode of the BLB, based on the use of the piezoelectric method of recording the signal in accordance with the scheme shown in figure 3.1.

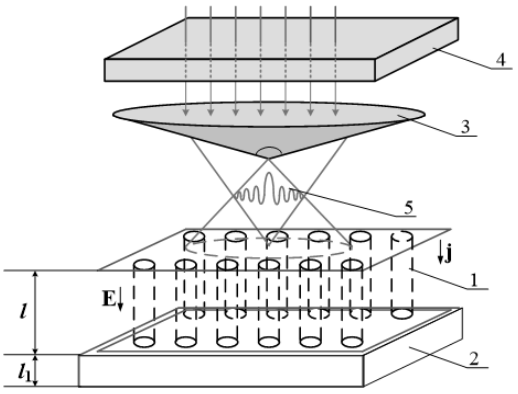

Figure 3.1. – The scheme of registration of a photoacoustic signal: 1 – the layer of chiral or achiral CNTs; 2 – piezoelectric detector; 3 – axicon; 4 – modulator; 5 – Bessel light beam

The simultaneous solution of the heat equation (2.1) and the equations for thermoelastic deformations in the sample and piezoelectric transducer l_1 allows us to find an expression for the photoacoustic signal. Assuming the boundaries of the "sample-piezoelectric detector" system to be free ($\sigma(l=0)=0$, $\sigma(l_1=0)=0$) and also using the technique described in [13], we will find the expression for the no-load voltage V^{TE} on a piezo transducer

$$V^{TE} = \frac{e}{\varepsilon^S}\left(U_P\big|_{z=l_1} - U_P\big|_{z=0}\right) = \frac{e}{\varepsilon^S}Z\,R^{TE}. \qquad (3.1)$$

In relation (1.5), the factor Z

$$Z = \frac{\sin^2\left(k_1\Delta l/2\right)}{m_0\sin k_1\Delta l\cos kl + \cos k_1\Delta l\sin kl} \qquad (3.2)$$

describes the purely acoustic properties of the "carbon nanotube-piezoelectric detector" system, and the factor R^{TE}

$$R^{TE} = \frac{\overline{E}^{TE}B_0k}{\left(\lambda_l+2\mu_l\right)k_S\sigma_S^2\alpha_{ef}}\left[\frac{1+\mu_1+\mu_2^2+\mu_3^2}{\left(1+\mu_1\right)\left(1+\mu_2^2\right)\left(1+\mu_3^2\right)}\right] \qquad (3.3)$$

determines the dissipative, dielectric, thermophysical, and thermoelastic properties of the sample under study, as well as the polarization and energy parameters of the BLB.

In the expressions (2.4), (3.1), (3.2) he following notation is introduced: $U(z)$, $U_p(z)$ are elastic displacements in the CNT layer and piezoelectric transducer; υ_{cn}, υ_p are values of velocities of elastic longitudinal waves, B_0 is the bulk modulus, $c^T = \lambda_l + 2/3\,\mu_l$, λ_l, μ_l are the Lame coefficients, a_0 is coefficient of volumetric thermal expansion, σ – values of elastic stresses, $\sigma_S = (1-i)a_S$, $a_S = (\Omega / 2\beta_{cn})^{1/2}$ is effective coefficient of thermal diffusion of the sample, β_{cn} is effective coefficient of sample thermal diffusivity, $\mu_1 = \alpha_{eff} / \sigma_S$, $\mu_2 = k / \sigma_S$, $\mu_3 = k / \alpha_{eff}$, $k_1 = \Omega / \upsilon_p$ is wave number of an elastic wave in a piezoelectric transducer, $k = \Omega / \upsilon_{cn}$ is wave number of a sound wave in a sample, $m_0 = (k_1 c^D) / (k c^T)$, $c^D = c^E(1 + e^2 / \varepsilon^S c^E)$, c^E is coefficient of rigidity of a piezoelectric, e – piezoelectric module, ε^S – dielectric constant of a piezoelectric crystal,

$$\overline{E}^{TE} = \eta\, a_t\, \alpha_{ef}\, E^{TE},\quad E^{TE} = A^{TE} / \left(\alpha_{ef}^2 - \sigma_S^2\right),$$

$$A^{TE} = \frac{2|\sigma_{cn}|I_0}{c\sqrt{\varepsilon'\varepsilon_0}}\frac{c}{4\pi}k_0\varepsilon_\alpha\left(n_1^2+n_2^2\right)\times$$

$$\times\left[\frac{m^2}{(q\rho)^2}J_m^2(qr)+J_m'^2(qr)\right],$$

$J_m'(q\rho) = \partial J_m(q\rho)/\partial\rho$ is derivative of the Bessel function J_m(q ρ) from the radial coordinate ρ. Analysis of expression (3.1) for the amplitude of the photoacoustic signal showed the presence of resonant peaks in the region of gigahertz frequencies (Figure 3.2).

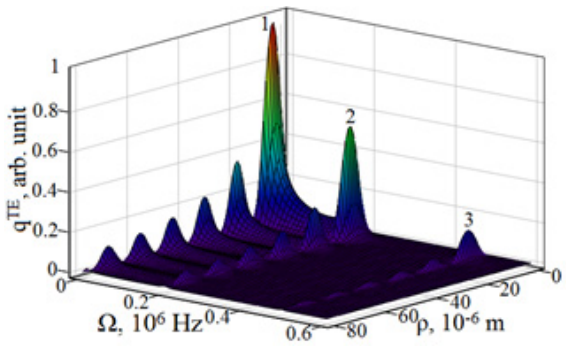

Figure 3.2 – Dependence of the amplitude of the PA signal on the radial coordinate and modulation frequency of the BLB ($m = 0$, $\alpha = 2^o$)

We note that we have considered a particular case of the free boundaries of the "sample-piezotransducer" system. In this case, the potential difference recorded by the detector is determined by the formulas (3.1)–(3.3). When the boundary conditions change, the relationships for calculating the potential difference appearing in the detector will change. Under conditions where the boundaries of the "sample-piezoelectric detector" system are fixed ($U(0) = 0$, $U(l + l_1) = 0$) or alternately loaded ($\sigma(0) = 0$, $U(l + l_1) = 0$; $\sigma(l + l_1) = 0$ $U(0) = 0$), other expressions for the potential difference are obtained. However, even in these particular situations, the main regularities of the photoacoustic transformation of the TE-mode of the BLB in magnetically low-dimensional structures correspond to those revealed on the basis of the model of free boundaries.

Using expression (3.1) for the idling voltage, it is possible to determine the amplitudes of photoacoustic signals for the system "sample-piezoelectric transducer" with alternately loaded boundaries:

$$\begin{cases}\sigma(l) = \sigma_p(l),\\ U(l) = U_p(l),\\ \sigma(0) = 0,\\ U_p(l_1) = 0,\end{cases} \tag{3.4}$$

$$\begin{cases}\sigma(l) = \sigma_p(l),\\ U(l) = U_p(l),\\ \sigma_p(l_1) = 0,\\ U(0) = 0.\end{cases} \tag{3.5}$$

The difference in the amplitude of the displacement of the boundaries of the system when the boundary conditions (3.4) is realized is determined by the following relation

$$U^{TE} = \frac{A_1'C_2' - A_2'C_1'}{A_1'B'_2 + A_2'B'_1}\left(e^{-2ik_1l_1}e^{ik_1l} - e^{-ik_1l}\right), \tag{3.6}$$

where

$$A_1' = 2k\,c^T\sin kl;\quad A_2' = 2\cos kl;$$

$$B_1' = ik_1c^D\left(e^{-2ik_1l_1}e^{ik_1l} + e^{-ik_1l}\right);$$

$$B_2' = \left(e^{-2ik_1l_1}e^{ik_1l} - e^{-ik_1l}\right);$$

$$C_1' = G_3'e^{ikl} - G_1';$$

$$C_2' = -\frac{iG_3'}{kc^T}e^{ikl} + G_2';$$

$$G_1' = E'B_0\alpha_t\left(\alpha_{eff}\left(\frac{\alpha_{eff}e^{-\alpha_{eff}l}}{\alpha_{eff}^2+k^2} - \frac{\sigma_S e^{-\sigma_S l}}{\sigma_S^2+k^2}\right) + \right.$$

$$\left. + \left(\frac{\alpha_{eff}}{\sigma_S}e^{-\sigma_s l} - e^{-\alpha_{eff}l}\right)\right);$$

$$G_2' = E'\frac{B_0\alpha_t\alpha_{eff}}{c^T}\left(\frac{e^{-\alpha_{eff}l}}{\alpha_{eff}^2+k^2} - \frac{e^{-\sigma_S l}}{\sigma_S^2+k^2}\right);$$

$$G_3' = E'B_0\alpha_t\left(\alpha_{eff}\left(\frac{\alpha_{eff}}{\alpha_{eff}^2+k^2} - \frac{\sigma_S}{\sigma_S^2+k^2}\right) + \left(\frac{\alpha_{eff}}{\sigma_S} - 1\right)\right);$$

$$E' = Q^{TE}\Big/\left(\alpha_{eff}^2 - \sigma_s^2\right);$$

$$c^D = c^E\left(1 + e^2\Big/\varepsilon^S c^E\right).$$

It is also easy to obtain an expression for the potential difference, taking into account the boundary conditions (3.5)

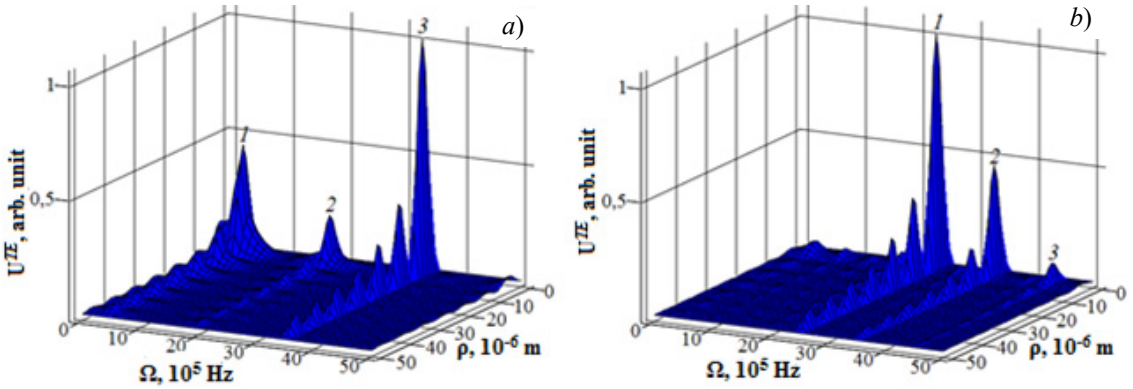

Figure 3.3 – Dependence of the amplitude of the photoacoustic signal U^{TE} on the radial coordinate when receiving the modulation frequency Ω: *a*) – the dependence under the boundary conditions (3.6); *b*) – dependence under the boundary conditions (3.7)

$$U^{TE} = \frac{A_1''C_2'' + A_2''C_1''}{A_1''B''_2 - A_2''B''_1} \times \times \left(2e^{-2ik_1l_1} - e^{-2ik_1l_1}e^{ik_1l} - e^{-ik_1l}\right), \quad (3.7)$$

where

$$A_2'' = 2i\cos kl; \quad A_2'' = 2i\sin kl;$$
$$B_2'' = \left(e^{-2ik_1l_1}e^{ik_1l} + e^{-ik_1l}\right);$$
$$B_1'' = ik_1c^D\left(e^{-2ik_1l_1}e^{ik_1l} - e^{-ik_1l}\right);$$
$$C_1'' = i\,k\,c^T G_3''e^{ikl} + G_1'';$$
$$G_2'' = G_2', \quad C_2'' = -G_3''e^{ikl} + G_2''; \quad G_1'' = G_1';$$
$$G_3'' = E'B_0\alpha_t\alpha_{eff}\left(\frac{1}{\alpha_{eff}^2 + k^2} - \frac{1}{\sigma_S^2 + k^2}\right).$$

Analyzing expressions (3.6) and (3.7), we see that the amplitude of the photoacoustic signal is determined in a rather complicated manner and depends on many parameters of the "sample-piezoelectric converter" system. In addition, the magnitude of the resulting signal is significantly affected by the modulating action of Bessel light beams (Figure 3.3).

As a result of the graphical analysis of expressions (3.6), (3.7), a resonant increase in the amplitude was detected.

It should be noted that the amplitude and position of the resonant peaks depend on the type of the boundary conditions imposed on the "sample-piezoelectric converter" system. At the same time, the tendency is generally to decrease the amplitudes of the resonance coordinates, as well as to identify and eliminate inconsistencies.

It can also be seen from the figures that an increase in the cone angle of a BLB affects the frequency of the appearance of resonant peaks as a function of the radial coordinate ρ. Controlling the amplitude of the resulting signal resulting from the modulated absorption of the light beam can be realized by using the taper angle adjustment schemes of the BLBs acting on the basis of the electrooptic Pockels effect [14], [15].

Thus, the model of photoacoustic transformation in the layer of chiral and achiral carbon nanotubes irradiated by the TE-mode of a Bessel light beam is constructed.

REFERENCES

1. *Thermooptical Sound generation by Bessel light beams in nonlinear crystals* / G.S. Mityurich [et al.] // International Journal of Thermophysics. – 2011. – Vol. 32, № 4. – P. 844–851.

2. *Bessel-beam Grueneisen relaxation photoacoustic microscopy with extended depth of field* / J. Shi [et al.] // Journal of Biomedical Optics. – 2015. – Vol. 20 (11). – p. 116002-1–116002-6.

3. Rapid three-dimensional isotropic imaging of living cells using Bes-sel beam plane illumination / T.A. Planchon [et al.] // Nature Methods. – 2011. – Vol. 8. – p. 417–423.

4. *Multicolor 4D fluorescence microscopy using ultrathin Bessel light sheets* / T. Zhao [et al] // Scientific Reports. – 2016. – Vol. 6. – P. 26159-1–26159-5.

5. *Trivedi*, *S*. Effect of vertically aligned carbon nanotube density on the water flux and salt rejection in desalination membranes / S. Trivedi, K.E. Alameh // SpringerPlus. – 2016. – Vol. 5 (1). – P. 1158-1–1158-13.

6. *Слепян*, *Г.Я*. Современные тенденции развития наноэлектро-магнетизма: аналит. обзор / НИУ «Ин-т ядерных проблем» БГУ; сост. Г.Я. Слепян, С.А. Максименко, П.П. Кужир. – Минск: Изд. центр БГУ, 2012. – 71 с.

7. *Stepanov*, *N.F*. Quantum mechanics and quantum chemistry / N.F. Stepanov. – M.: Mir, 2001. – 519 p.

8. *Mintmire*, *J.W*. Electronic and structural properties of carbon nanotubes / J.W. Mintmire, C.T. White // Carbon. – 1993. – Vol. 33, № 7. – P. 893–902.

9. *Maksimenko*, *S.A*. Electrodynamics of carbon nanotubes / S.A. Maksimenko, G.Ya. Slepyan // Radio engineering and electronics. – 2002. – Vol. 47. – P. 261.

10. *Митюрич*, *Г.С.* Фотодефлекционный сигнал, генерируемый бесселевым световым пучком в плотном слое углеродных нанотрубок / Г.С. Митюрич, Е.В. Черненок, А.Н. Сердюков. // Проблемы физики, математики и техники. – 2015. – № 4 (25). – С. 20–27.

11. *Saito*, *R*. Physical properties of carbon nanotubes / R. Saito, M.S. Dresselhaus, G. Dresselhaus. – London: Imperial College Press, 1999. – 251 p.

12. *Mintmire*, *J.W*. Electronic and structural properties of carbon nano-tubes / J.W. Mintmire, C.T. White // Carbon. – 1995. – Vol. 33, iss. 7. – P. 893–902.

13. *Photoacoustic transformation of Bessel light beams in magnetoactive superlattices* / G.S. Mityurich, E.V. Chernenok, V.V. Sviridova, A.N. Serdyukov // Crystallography Reports. – 2015. – Vol. 60, № 2. – P. 273–279.

14. *Устройство управляемой термооптической генерации акустической волны*: пат. 10757u Респ. Беларусь, МПК (2006.01) G10K 11/00 / Г.С. Митюрич, Е.В. Черненок, А.Н. Сердюков; заявитель ГГУ им. Ф. Скорины. – № u 20150083; заявл. 09.09.2015; опубл. 30.09.2015 // Афіцыйны бюл. / Нац. цэнтр інтэлектуал. уласнасці. – 2015. – № 4. – С. 146.

15. *Устройство управляемой лазерной генерации звука*: пат. 11032u Респ. Беларусь, МПК (2006.01) G10K 11/00 / Г.С. Митюрич, Е.В. Черненок, А.Н. Сердюков; заявитель ГГУ им. Ф. Скорины. – № u 20150378; заявл. 06.11.2015; опубл. 30.04.2016 // Афіцыйны бюл. / Нац. цэнтр інтэлектуал. уласнасці. – 2016. – № 2. – С. 162–163.

Поступила в редакцию 20.10.2020.